Three-Dimensional Simulation Study of Spheromak Injection into Helical Plasmas

SUZUKI Yoshio*, WATANABE Tomohiko, KAGEYAMA Akira, SATO Tetsuya,
HAYASHI Takaya and the Complexity Simulation Group
National Institute for Fusion Science, Toki 509-5292, Japan

Abstract

Three-dimensional dynamics of a spheromak, which is injected into a magnetized target plasma is investigated by using magnetohydrodynamic (MHD) numerical simulations. It is found that the process of the spheromak penetration is much more complicated than what has been analized so far by using a simple conducting sphere model. Namely, the injected spheromak suffers from the tilting instability, which grows with the similar time scale as the penetration of the spheromak. The instability is accompanied by magnetic reconnection between the spheromak field and the target plasma field, by which the magnetic configuration of the spheromak is disrupted. As a result, the high density plasma confined in the spheromak field is supplied in the target plasma region. It is found that the magnetic reconnection suppresses the penetrating motion of the high density plasma. The kinetic energy of the injected spheromak is lost also through an excitation of convection and compressional heating in the target plasma. It is also found that the density and the pressure of the target plasma are important in determining the transfer rate of the kinetic energy of the spheromak. This rate is directly related to the depth of the penetration before the spheromak is disrupted.

Keywords:

1. Introduction

For steady state operation of a fusion device, several fueling schemes have developed. However, conventional schemes such as gas puffing and pellet injection are not expected to fuel deeply reactor grade plasmas. The spheromak injection is one of the most promising schemes for deep fueling and has been discussed in several theoretical models [1-3] and experiments [4-6]. Our main objective is to investigate the dynamics of the injected spheromak as well as the possibility of deep fueling. To achieve this, we study three-dimensional dynamics of a spheromak which is accelerated by a spheromak gun and is injected into a magnetized target plasma by using magnetohydrodynamic (MHD) numerical simulations. We assume that a plasma in a fusion device is modelled by the target plasma. In the following, therefore, the target plasma will be called the device plasma.

2. Simulation Model

In this study, we use cylindrical coordinates (r, θ, z). The simulation region is composed of two cylinders which connect with each other (Figure 1). One with a smaller radius L_r corresponds to a spheromak gun region and the other with a larger radius $4L_r$ is a part of the fusion device region. Lengths of these cylinders are both $L_z/2$. The relative lengths of the sizes are given by $L_r:L_z = 1:16$. We employed a perfectly conducting wall for the boundary condition.

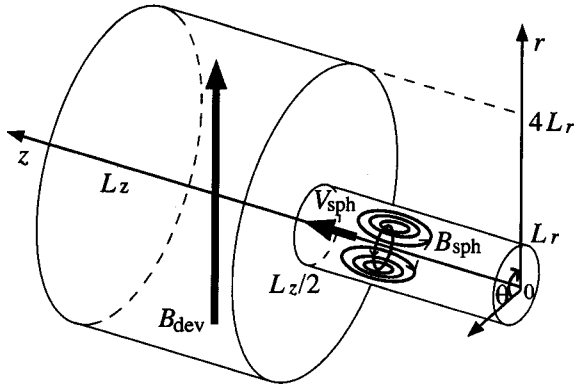*Corresponding author's e-mail: suzuki@toki.theory.nifs.ac.jp

Fig. 1 Schematic diagram of the simulation region.

Table 1 Several parameters in four different simulation runs.

	spheromak			device		common
case	B_{sph}	ρ_{sph}	V_{sph}	B_{dev}	ρ_{dev}	P_{com}
1	1	10	0.3	0.1	1	0.4
2	1	10	0.3	0	1	0.4
3	1	10	0.3	0	0.1	0.4
4	1	10	0.3	0	0.1	0.1

The governing equations are given by MHD equations:

$$\frac{\partial \rho}{\partial t} = - \nabla \cdot (\rho V),$$

$$\frac{\partial \rho V}{\partial t} = - \nabla \cdot \rho VV + J \times B - \nabla P - \nabla \cdot \hat{\Pi},$$

$$\frac{\partial B}{\partial t} = - \nabla \times E,$$

$$\frac{\partial P}{\partial t} = - \nabla \cdot (PV - \kappa \nabla T) - (\gamma - 1)(P \nabla \cdot V + \hat{\Pi} : \nabla V - \eta J^2),$$

$$E = - V \times B + \eta J,$$

$$J = \nabla \times B,$$

$$\hat{\Pi} = \nu \left[\frac{2}{3} (\nabla \cdot V) \hat{I} - \nabla V - {}^t(\nabla V) \right].$$

These equations have a non-dimensional form, in which the density, the magnetic field, the velocity, the length, and the time are normalized by one-tenth of the maximum spheromak density $\rho_0 (\equiv 0.1 \rho_{sph})$, the maximum strength of the spheromak magnetic field B_{sph}, the characteristic Alfvén speed $V_A (\equiv B_{sph}/\sqrt{\mu_0 \rho_0})$, the scale of the cylinder radius L_r and the Alfvén transit time $\tau_A (\equiv L_r/V_A)$, respectively. The resistivity η, the viscosity ν, and the conductivity κ are fixed to 1.0×10^{-3} in the normalized unit $\mu_0 L_r V_A$, $\rho_0 L_r V_A$, and $k \rho_0 L_r V_A$ respectively.

The initial magnetic configuration is calculated as follows: The toroidal current J_θ of a cylindrical spheromak solution [7] whose radius and length are respectively L_r and $2L_r$ is located in the injection region (Its center is at $z = 6L_r$). From J_θ, the toroidal vector potential A_θ, and thus the magnetic field is calculated.

Furthermore, the current free field B_{dev}, whose direction is an almost uniform and perpendicular to the injection direction is superposed. The density profile is given by the function of the poloidal flux ψ_{pol} which is defined by rA_θ,

$$\rho = \rho_{dev} + (\rho_{sph} - \rho_{dev}) \frac{\psi_{pol}}{\psi_{axis}},$$

where ψ_{axis} is the poloidal flux on the spheromak magnetic axis. In this paper, the device plasma density ρ_{dev} is assumed to be 0.1 or 0.01 times lower than the peak spheromak plasma density ρ_{sph}. The pressure is initially uniform ($P_{com} = P_{dev} = P_{sph}$). The spheromak is injected into the device region after acceleration up to the maximum velocity V_{sph} at $t = 2L_r/V_{sph}$.

We carry out four simulation runs as shown in Table 1. The explicit finite difference method with second-order accuracy and the Runge-Kutta-Gill method are used to solve the basic equations numerically.

3. Simulation Results

Figure 2 shows the time evolution of the spatial structure of magnetic field lines and the high density plasma in the case 1. From this figure, we can see that the spheromak field which confines the high density plasma penetrates into the device region, but it suffers from the tilting instability ($t = 0$, 20 τ_A). The magnetic moment of the spheromak is initially directed to $-z$, and the device field is directed from $\theta = 3/2\pi$ to $\theta = \pi/2$. Thus, the spheromak tilts to align its magnetic moment to the direction of the device field [8]. In this process the magnetic reconnection between the spheromak field and the device field takes place in front of the spheromak ($t = 20$ τ_A). At $t = 40$ τ_A, the magnetic configuration of the spheromak is almost disrupted. At $t = 60$ τ_A, the high density plasma confined in the spheromak field diffuses in the device region. The magnetic reconnection plays a role to supply the high density plasma into the device region.

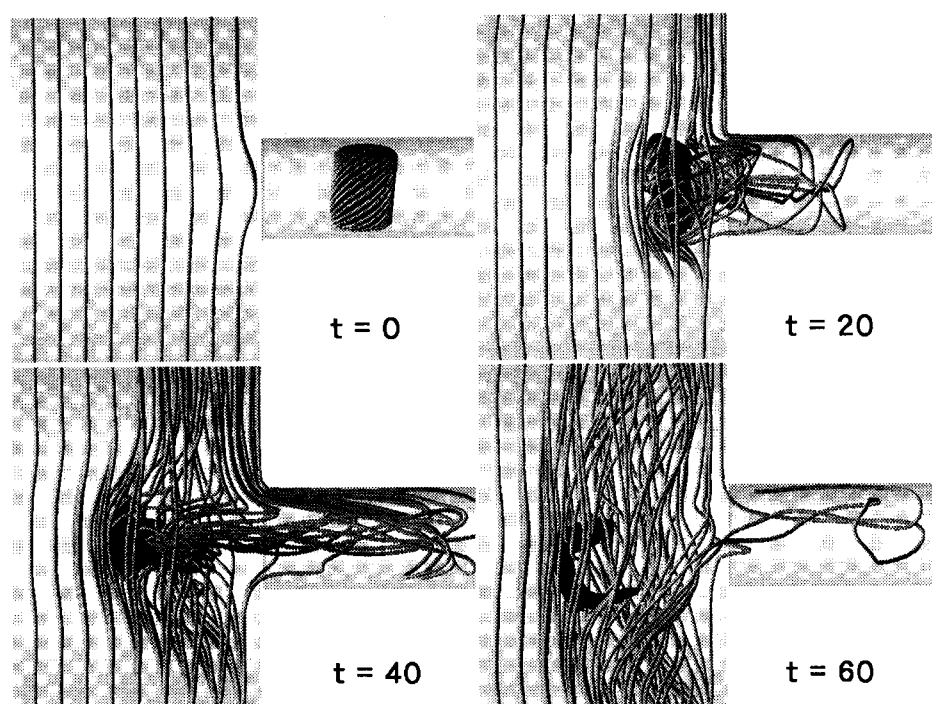Figure 3 shows the time evolution of the penetration depth of the spheromak high density plasma (L_p),

Fig. 2 The spatial structure of the magnetic field lines and the high density plasma (black region) viewed from $\theta=0$ at $t=0$, 20, 40, and 60 τ_A for the case 1. The region shown here is magnified.

which is defined by,

$$L_p = \frac{\int_{\rho>\rho_c} \rho z \mathrm{d}V}{\int_{\rho>\rho_c} \rho \mathrm{d}V} - L_z/2 ,$$

where $\rho_c = \rho_{sph}/2$. In the case 1, the spheromak high density plasma enters the device region at $t=12\tau_A$ and penetrates with time. However, after about $t=30\tau_A$, the penetration depth becomes shorter than that in the case 2, where the device fild B_{dev} is assumed to be null. As shown in figure 2, the reconnection process successively proceeds around $t=20\tau_A$. It means that the magnetic reconnection suppresses the penetrating motion of the spheromak high density plasma. The suppression of the penetration by the reconnection process may be caused by both of a drag force of the plasma mass which the reconnected magnetic fields are frozen in, and a drag force of the magnetic tension of the reconnected field lines.

In this figure, results of the case 3 and the case 4 are also shown. In the case 3, where the device density is one-tenth of the case 2, the penetration depth is longer. In this case, the kinetic energy of the spheromak is less transferred to the device plasma convection. In the case 4, where the device density is same as in the case 3 but the initial pressure is one-fourth of the case 3, the penetration depth is much longer. In this case,
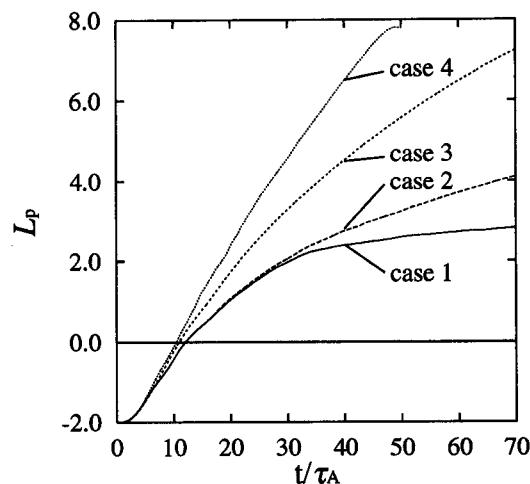

Fig. 3 Time evolution of the penetration depth of the spheromak high density plasma. (The region $0 \le L_p \le 8$ corresponds to the device region.)

the energy conversion to the thermal energy by the compressional heating is smaller than in the case 3. These results clearly indicate that the density and the pressure of the device plasma are important in determining the transfer rate of the kinetic energy of the spheromak, and that the rate is directly related to the depth of the penetration before the spheromak is

disrupted due to the tilting instability. For the lower device density and the lower pressure, the penetration depth is longer.

4. Discussion

Let us compare the simulation results with the simple conducting sphere model, in which an incompressible, perfectly conducting sphere is injected into a vacuum magnetic field increasing along the injection direction[6]. This model indicates that the sphere can penetrate until the initial kinetic energy of the sphere is exceeded by the magnetic energy required to exclude magnetic field from the sphere volume. In the simulations the initial kinetic energy is given by $<\rho_{sph}> V^2_{sph}/2$, where $<\rho_{sph}>$ is the average spheromak density and is about 4. Because the injection velocity is 0.3, the initial kinetic energy is about 0.18. It means that the spheromak can penetrate until the device magnetic field becomes 0.6. Although the device field in the case 1 is 0.1, the penetration depth is saturated. In this case, the penetrating motion is suppressed by the magnetic reconnection as well as the excitation of the device field convection, which are not considered in the simple conducting sphere model.

Let us compare the simulation parameters with the LHD experiments. If we take the radius of the gun region L_r to 0.15 m, $L_z/2$ becomes 1.2 m, which corresponds to the plasma diameter of LHD. For the spheromak parameters, if we take the density ρ_{sph} to 1×10^{-5} kg/m^3 and the maximum strength of the magnetic field B_{sph} to 1 T, the Alfvén velocity V_A is 690 km/s. Thus, the injection velocity V_{sph} is 207 km/s. For the device parameters, the density ρ_{dev} in the case 1 and the case 2 is 1×10^{-6} kg/m^3, and in the case 3 and the case 4 it is 1×10^{-7} kg/m^3. In the case 4, the initial pressure P_{com} is lower and corresponds to 5 keV in terms of temperature. Therefore parameters used in the case 4 is close to the LHD experiments except for the strength of the device field. Therefore, it is expected that the loss of the spheromak kinetic energy by the device plasma convection is as well as the compressional heating less in the real experiment. Also, in the case 1 the strength of the magnetic field B_{dev} is 0.1, which corresponds to 0.1 T. It means that although the device field in the present simulation is much weaker than in the real experiment, the reconnection process influences the penetration depth. In our simulation, the dependence on the device field strength as well as the injection velocity is not considered. It will be reported in a future work.

5. Summary

When the spheromak is injected into the magnetized plasma region, the magnetic reconnection between the spheromak field and the device field takes place. Because the reconnection process proceeds successively, the magnetic configuration of the spheromak is disrupted. As a result, the high density plasma is supplied in the device region. Also, from the search of the penetration depth of the spheromak high density plasma, the magnetic reconnection is found to suppress the penetrating motion. Furthermore, the values of the density and the pressure of the device plasma are found to give significant influence on the penetration depth of the spheromak. The process of the penetration of the injected spheromak is much more complicated than an estimation based on a simple conducting sphere model, because several events like the growth of the tilting instability, the occurrence of the magnetic reconnection, and the excitation of convection in the device plasma take place simultaneously with similar time scales. In order to study in detail the dependence on the strength of the device field as well as the injection velocity should be considered.

References

[1] P.B. Parks, Phys. Rev. Lett. **61**, 1364 (1988).
[2] L.J. Perkins, S.K. Ho and J.H. Hammer. Nucl. Fusion **28**, 1365 (1988).
[3] W.A. Newcomb, Phys. Fluids B **3**, 1818 (1991).
[4] R. Raman *et al.*, Phys. Rev. Lett. **73**, 3101 (1994).
[5] M.R. Brown and P.M. Bellan, Nucl. Fusion **32**, 1125 (1992).
[6] M.J. Gouge *et al.*, *Proc. of the 16th IAEA Fusion Energy Conference*, Montréal, Canada, October 1996.
[7] J.M. Finn and W.M. Manheimer, Phys. Fluids **24**, 1336 (1981).
[8] T. Sato and T. Hayashi, Phys. Rev. Lett. **50**, 38 (1982).